Multiple-Spin Exchange on a Triangular Lattice: A Quantitative Interpretation of Thermodynamic Properties of Two-Dimensional Solid ^{3}He

M. Roger,[1] C. Bäuerle,[2] Yu. M. Bunkov,[2] A.-S. Chen,[2] and H. Godfrin[2]

[1]*Service de Physique de l'Etat Condensé, Commissariat à l'Energie Atomique, Centre d'Etudes de Saclay,
91191 Gif sur Yvette Cedex, France*
[2]*Centre de Recherches sur les Très Basses Températures, Centre National de la Recherche Scientifique, BP 166,
38042 Grenoble Cedex 9, France*

(Received 11 September 1997)

We apply exact high-temperature series expansions of the multiple-spin-exchange Hamiltonian for a triangular lattice to describe high precision NMR measurements of the nuclear magnetic susceptibility of ^{3}He films adsorbed on graphite, reported here, as well as all available specific heat data. A consistent quantitative description of the unusual thermodynamic properties of the second layer solid, which provides canonical examples of two-dimensional magnets, is obtained as a function of temperature and areal density. We prove that cyclic multiple-spin exchange processes are responsible for the large degree of frustration found in the antiferromagnetic phase and that they remain significant in the ferromagnetic phase. [S0031-9007(97)05249-6]

The microscopic theory of magnetism for a system of almost localized identical fermions is based on the concept of permutations of particles (cf. the elegant formalism developed by Dirac [1]). The most general expression for an effective exchange Hamiltonian is $\mathcal{H}_{ex} = -\sum_P (-1)^p J_P P$ where the sum is over all permutations P (with parity p) of the symmetric group acting on spin variables [1,2]. It reduces to the Heisenberg Hamiltonian when only pair transpositions are retained, i.e., when two-particle exchange dominates, as generally found in electronic magnets. Thouless [2] stressed the importance of higher order interactions—as cyclic three- and four-particle exchange—in a hard-core quantum solid like solid ^{3}He. He pointed out that even permutations like cyclic three-particle exchange generally lead to ferromagnetism, while odd permutations like two or cyclic four-particle exchange favor antiferromagnetism (i.e., all J_P are positive). These predictions have been verified in bulk solid ^{3}He [3] which is well described by the multiple-spin exchange (MSE) model [4].

Delrieu gave convincing arguments for the predominance of ferromagnetic three-particle exchange in closed packed lattices like the three-dimensional (3D) hcp phase of solid ^{3}He or the two-dimensional (2D) triangular lattice in high density ^{3}He films [5]. In low density films, higher order antiferromagnetic exchanges like four- and six-spin exchange were expected to compete with ferromagnetic three-spin exchange, as is observed in the loose packed 3D bcc phase [4].

Recent *ab initio* quantum Monte Carlo calculations of various exchange frequencies for a ^{3}He monolayer have corroborated the MSE picture [6]: the relevant processes are cyclic exchanges J_n involving the most symmetric rings of n nearest neighbors, with $n = 3, 2, 4, 6,$ and 5 by decreasing amplitude (Fig. 1). Note that the MSE parameters are expected to depend strongly on the areal

density ρ. From experimental measurements on submonolayer films [7] and theoretical calculations [8], values of the order of 25 can be estimated for the Grüneisen parameter $\Gamma_J = -d \ln(J)/d \ln(\rho)$.

From the experimental point of view, the second solid layer of ^{3}He films adsorbed on graphite is a particularly interesting magnetic system, discussed in detail in recent publications [9,10]. A large exchange coupling J between the nuclear spins is observed (several mK), which evolves from antiferromagnetism to ferromagnetism as a function of density. The first layer only plays the role of an inert substrate, since exchange is practically inhibited due to its very high density. The second layer completely solidifies before third layer promotion, forming a commensurate phase with respect to the first layer with a 4/7 ratio of densities. It is characterized by an antiferromagnetic Curie-Weiss susceptibility, and by a large heat capacity at low temperatures with a weak temperature dependence. In the presence of a partial liquid third layer the system becomes ferromagnetic, the effect being particularly large at the "ferromagnetic peak" close to promotion in a fourth layer. The Heisenberg model has been often found adequate to fit the susceptibility and heat capacity of these systems, a fact which is *a priori* at variance with the MSE description. However, the Heisenberg exchange parameter J deduced from heat capacity differs from the value found in susceptibility experiments, suggesting that MSE could indeed play an important role [9].

The microscopic mechanism giving rise to the strong antiferromagnetism of the low density second layer can
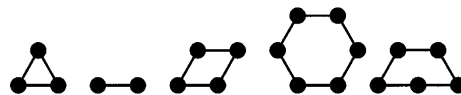

FIG. 1. Relevant exchange cycles in 2D solid ^{3}He.

certainly be ascribed to multiple-spin exchange processes [9,11,12]. However, there is presently no firm conclusion regarding the nature of the interactions in the ferromagnetic regime and in the intermediate region. In particular, the presence of the liquid in the partially filled third layer allows a Rudermann-Kittel interaction which could explain the ferromagnetism of these films [9].

In order to understand quantitatively the physics of ^{3}He films, we apply the exact high temperature series expansions (HTSE) of the MSE Hamiltonian calculated recently [13] to analyze thermodynamic measurements: available heat capacity data [10,12] and the present very high precision magnetic susceptibility measurements. Note that fits of the susceptibility by HTSE require high accuracy data since the trivial $1/T$ dependence must be removed. A run at submonolayer coverages, where the susceptibility is given by a Curie law and proportional to the number of atoms, allows us to establish a reliable calibration for the susceptibility measurements. The sample temperature is determined by a melting curve thermometer in the range 4 to 300 mK. The ^{3}He nuclear susceptibility is measured by continuous-wave NMR at a frequency of 511.3 kHz. In the present work the uncertainty, typically of order 2%, is dominated by systematic errors in the integration of the wings of the NMR lines. Further details are given elsewhere [14].

Coverages, expressed in "layers," are defined as the ratio x between the total number of adsorbed ^{3}He atoms to that in the densest (saturated) first layer. The latter has an areal density of 11.09 atoms/nm^2 according to neutron diffraction measurements. We have measured 26 coverages for $1.55 < x < 2.4$, i.e., from second layer solidification to high multilayer coverages.

For the MSE HTSE fits we consider the Hamiltonian:

$$\mathcal{H}_{\text{ex}} = J \overset{(2)}{\sum} \mathcal{P}_2 + J_4 \overset{(4)}{\sum} \mathcal{P}_4 - J_5 \overset{(5)}{\sum} \mathcal{P}_5 + J_6 \overset{(6)}{\sum} \mathcal{P}_6 . \tag{1}$$

The sums correspond, respectively to cyclic 2, 4, 5, and 6-particle permutation operators (Fig. 1) acting on spin variables. Cyclic n-particle exchanges, with n odd can be expressed in terms of $(n - 1)$-particle exchanges [2]. Three particle exchange J_3 is incorporated in an effective pair exchange constant: $J = J_2 - 2J_3$. We have not reexpressed five-spin exchange in terms of two- and four-spin exchanges; this leads to an effective four-spin exchange constant $K = J_4 - 2J_5$ for the most symmetric four-spin cycles (Fig. 1) plus the contribution of other four-spin cycles and pair exchange with third neighbors. Since the dominant part of possible indirect interactions between the solid second layer and the fluid third layer can be reduced to an effective Heisenberg interaction J_{RKKY} between first neighbors in the second layer [9], they are easily incorporated in our Hamiltonian with $J = J_2 - 2J_3 - J_{\text{RKKY}}$.

Using the cluster method, we have generated HTSE up to order 5 in $\beta = 1/k_B T$ for the specific heat and spin susceptibility [13]. Close to the ferromagnetic Heisen-berg model (J negative and dominant), the behavior of the susceptibility series is improved by an Euler transformation $\beta = u/(1 - u)$. The series $f = \chi T$ are then analyzed through differential approximants [15]. We write: $Q(u)uf'(u) + P(u)f(u) = R(u)$. $Q(u) = (1 - u)^2$ and $P(u) = 3 - (\gamma + 3)u$ are chosen to recover the expected low temperature behavior $\chi T \approx T^3 \exp(\gamma/k_B T)$ [16]. At order n, γ and the n coefficients of the $(n - 1)$th-order polynomial $R(u)$ are obtained by writing that the previous equation is verified up to order n. The differential approximant DA$[n]$ is the solution that tends to 1 for $u \to 0$. For the ferromagnetic Heisenberg model, those approximants converge nicely at low temperature to the best estimates from renormalization group techniques [16] and give an excellent interpolation between low and high temperature behavior [17]. We have also used usual Padé approximants [15] after the same Euler transformation for susceptibility and specific heat series. A $[L, M]$ Padé approximant to the series $A(\beta)$ is a rational fraction P_L/Q_M, with P_L and Q_M, polynomials of degree L and M in β, satisfying: $A(\beta) = P_L/Q_M + O(\beta^{L+M+1})$. We consider that the series are reliable down to temperatures where different approximants differ by more than 5%.

Using heat capacity, neutron scattering, and the present susceptibility data at high temperatures, we determined the second layer density $\rho_2(x)$ [18] with more precision than in previous attempts [10]. For the MSE fits we use four parameters: the Heisenberg term $J = J_2 - 2J_3$, the effective four-spin exchange constant $K = J_4 - 2J_5$, and the ratios $\eta = J_5/J_4$ and $\nu = J_6/J_4$. Other quantities of interest, given by different combinations of the exchange parameters [6], are J_c, the leading term in specific heat data $[C_s = 9n_2 k_B (J_c\beta)^2/4]$, and J_χ defined as $\theta/3$, where θ is the Curie-Weiss temperature.

We first fit HTSE of $C_s(T)$ to the data obtained by Greywall [10] at the coverages $x = 1.61, 1.75, 1.84, 1.93, 2.02, 2.11, 2.19$, and 2.28. The results are shown in Fig. 2. As already stressed [13], the thermodynamic data are very sensitive to K, and a little less to ν but the influence of η is weak as long as K remains positive ($\eta < 0.5$). Values of η in the range $0.2 \lesssim \eta \lesssim 0.4$ yield fits of comparable quality, the optimum being $\eta = 0.35$ for $x = 1.61$ and $\eta = 0.3$ for all other coverages. The other parameters of the fit are shown in Fig. 4 (filled symbols). J and K are determined with good accuracy (5% to 10%). There is a larger dispersion ($\approx 20\%$) on ν. The weak dependence of η and ν on density is consistent with the fact that J_4, J_5, and J_6 have the same order of magnitude.

We have measured in the same density range the total susceptibility $\chi(T)$ for 17 coverages:

$$\chi(T) = (\gamma\hbar/2)^2$$
$$\times [n_1 + n_2 f(T) + n_3/\sqrt{1 + (T_F/T)^2}]/k_B T ,$$

where n_i is the number of atoms in layer i. The three terms represent, respectively, the contribution of the paramagnetic first layer, the exchange contribution of the second layer with $f(T)$ given by approximants to the
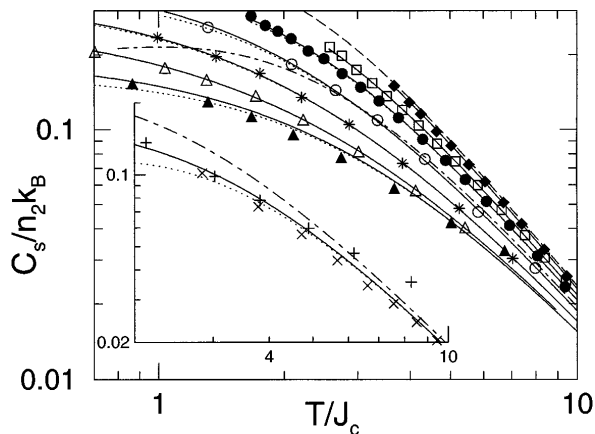
FIG. 2. MSE fits of the specific heat data of Greywall, at coverages (from bottom to top) $x = 1.75$, 1.84, 1.93, 2.02, 2.11, 2.19, and 2.28. The inset shows data of Greywall ($+$) and Siqueira *et al.* ($\times$) at $x = 1.61$ (commensurate phase). The full and dotted lines represent, respectively, [2,3] and [3,2] Padé approximants after an Euler transformation (cf. text). For comparison, we have also represented the specific heat for the ferromagnetic (dashed line) and antiferromagnetic (dash-dotted lines) Heisenberg model.

FIG. 3. MSE fits of the second layer susceptibility. The upper part represents data at $x = 2.02$ (∗), $x = 2.07$ ($+$), and $x = 2.09$ (●). The lower part shows data at $x = 1.55$, 1.62, 1.66, 1.71, 1.76, 1.90, and 1.94 from bottom to top. The solid lines represent DA [5] differential approximants in the ferromagnetic regime and [3,2] Padé approximants elsewhere. The dotted lines represent [3,2] ([2,3]) Padé approximants in the ferromagnetic regime (elsewhere).

HTSE, and the contribution of the liquid third layer taken from recent data on ^{3}He films [14]. The susceptibility is less sensitive than the specific heat to the influence of each exchange frequency and it is impossible to determine the four unknown parameters independently. For each curve, we proceed as follows: (i) We take $\eta = 0.3$ for $x > 1.7$ and $\eta = 0.35$ below this coverage (same as above); (ii) we fix J_c from the interpolation of the values obtained from the specific heat data; (iii) the remaining parameters K/J and ν are then determined without ambiguity. The results are shown in Fig. 3. The parameters of the fits, given in Fig. 4 (open symbols), are found to agree remarkably well with the values deduced from the specific heat when MSE is important ($|K/J| \gtrsim 0.07$). Closer to the pure Heisenberg behavior, it is impossible to deduce precise values of K/J and ν from the susceptibility data.

It is of importance to examine the effect of the finite size (≈ 10 nm) of the graphite platelets. If we assume a proportion of order 10% [9] of paramagnetic spins localized on the platelets edges we fit the data with MSE frequencies changed by a comparable amount, but the general behavior is not affected. The results will be published elsewhere.

Several important new features arise from the MSE analysis. A pure Heisenberg behavior $J_c \approx J_\chi$ (MSE negligible) is only recovered at $x > 2.2$. The parameters $|J|$, J_c, J_χ rise monotonously when x decreases down to $x_0 \approx 1.8$, a value substantially lower than that corresponding to the "ferromagnetic peak": $x_p \approx 2$, identified in fits based on a Heisenberg model [9]. Indeed, at $x \approx x_0$, a kink in the second-layer melting temperature $T_m(x)$ has been reported [19], suggesting a structural change in the second layer.
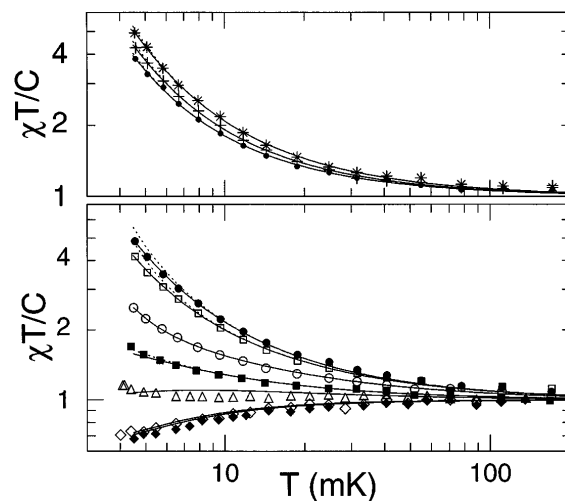
At $x \approx x_0$ the effective pair exchange $J \approx -12$ mK is ferromagnetic with a magnitude 3.5 times larger than J_c. However, the specific heat is lower than that corresponding to an antiferromagnetic Heisenberg model and comparable to that observed in the antiferromagnetic commensurate phase (see Fig. 2). This means that we have a puzzling *highly frustrated ferromagnetic phase*. Further experimental investigations near $x \approx x_0$ are encouraged.

In all that coverage range, $|J|$ and J_c vary exponentially as a function of the second layer density ρ_2 (cf. inset of Fig. 4) with respective Grüneisen constants $\Gamma_J = 34$ and $\Gamma_{J_c} = 26.5$ [20]. These values are in good agreement with theoretical predictions using WKB approximations [8] and NMR measurements on submonolayer films [7]. They can also be compared to the value $\Gamma_{J3D} \approx 18$ obtained in the 3D solid [4]: assuming that exchange frequencies mainly depend on the interatomic distance, we indeed expect $\Gamma_J \approx \frac{3}{2} \times \Gamma_{J3D} \approx 27$. Hence, there is a remarkable continuity in the exponential behavior of the exchange parameters from the highest coverages, down to $x \approx 0.18$ with no indication of structural changes in the incommensurate second layer. Moreover, the fact that the density dependence of the exchange frequencies is that expected within a MSE model is a strong indication that interlayer exchanges (J_{RKKY}) are not important. This conclusion is reinforced by the fact that for $x \to x_0+$, $|K/J|$ increases; if the abrupt rise of the effective pair exchange constant $-J$ was due to the occurrence of interlayer exchange, we would observe a Heisenberg behavior with an abrupt decrease of $|K/J|$.

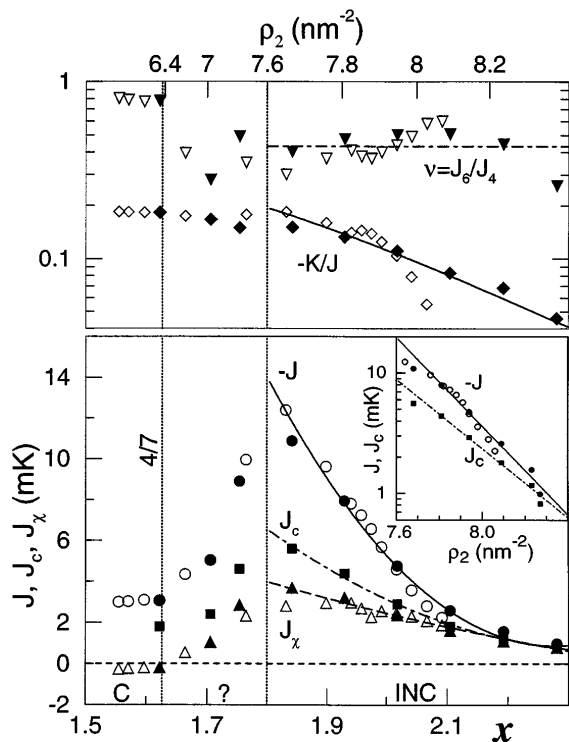At low coverages, near the second-layer solidification, the exchange frequencies are practically constant

FIG. 4. MSE parameters J ($\bigcirc$), J_c ($\square$), J_χ ($\triangle$), $-K/J$ ($\diamond$) and ν (∇) in terms of coverage x. Filled symbols (open symbols) are deduced from specific heat (susceptibility) fits. The curves are least square fits to various parameters in the incommensurate phase. The inset is a semilog plot of J, J_c as a function of the second layer density ρ_2. Commensurate (C), incommensurate (INC), and intermediate (?) phases are indicated on the x axis.

in the range $1.55 < x < 1.62$. Surprisingly, we obtain very small values for the Curie-Weiss temperature ($J_\chi \approx -0.2$ mK), showing that the "antiferromagnetic behavior" found in a Heisenberg description of susceptibility data is probably governed by MSE corrections. This system displays therefore a very interesting case of frustration. The value of $-J = 2J_3 - J_2$ is much lower than near $x = x_0$, in the incommensurate solid, suggesting that J_2/J_3 is much larger, thus leading to a strong compensation in J. Several reasons may explain the larger relative value of J_2: (i) The very low density; (ii) in the absence of a dense third layer, the excursion of atoms in the direction perpendicular to the plane during exchange processes is important and might favor pair exchange with respect to three-particle exchange [6].

At $x = 1.62$ the density of the solid second layer is $4/7$ of the first layer density and the fraction of liquid is $x_3 = 0.06$. At $x = 1.55$ the amount of solid in the second layer decreases by about 10%. This is consistent with the coexistence of commensurate solid with some fluid, in agreement with Ref. [10].

The transition region ($1.62 < x < 1.8$) remains challenging. We find that the second-layer density varies by 1.2 nm^{-2} while the third-layer density increases only by 0.6 nm^{-2}, strongly suggesting a rearrangement of the

second layer with a possible coexistence of commensurate and incommensurate phases. Indeed, if we assume a phase coexistence we obtain, at a special coverage $x \approx 1.66$ where the sign of J_c is changing, better susceptibility fits than that represented in Fig. 3 ($\triangle$) [18].

The experimental and theoretical results presented in this article demonstrate the importance of multiple spin exchange processes over a wide density range in adsorbed ^{3}He films, the only experimental examples of low-dimensionality nuclear magnets known presently. Quantitative agreement is obtained in the description of different thermodynamic properties in the high temperature range covered by series expansions of the multiple-spin-exchange Hamiltonian. The system exhibits a remarkable evolution from antiferromagnetism to ferromagnetism as the density increases, with the extraordinary feature that both states are highly frustrated. Its unusual properties raise challenging questions on the nature of frustrated magnets at very low temperatures. Understanding the ground state of the MSE model will require further theoretical work. In particular, detailed quantum Monte Carlo calculations of multiple-spin-exchange frequencies would be extremely valuable, since they would provide an independent test of the model.

[1] P. A. M. Dirac, *The Principles of Quantum Mechanics* (Clarendon, Oxford, 1947).

[2] D. J. Thouless, Proc. Phys. Soc. **86**, 893 (1965).

[3] D. D. Osheroff, J. Low Temp. Phys. **87**, 297 (1992).

[4] M. Roger, J. H. Hetherington, and J. M. Delrieu, Rev. Mod. Phys. **55**, 1 (1983).

[5] J. M. Delrieu *et al.,* J. Low Temp. Phys. **40**, 71 (1980).

[6] B. Bernu, C. Lhuillier, and D. Ceperley, J. Low Temp. Phys. **89**, 589 (1992); private discussions.

[7] M. Richards, in *Phase Transitions in Surface Films,* edited by J. G. Dash and J. Ruvald, NATO Advanced Study Institutes, Ser. B, Vol. 51 (Plenum, New York, 1980).

[8] M. Roger, Phys. Rev. B **30**, 6432 (1984).

[9] H. Godfrin and R. E. Rapp, Adv. Phys. **44**, 113 (1995).

[10] D. S. Greywall, Phys. Rev. B **41**, 1842 (1990).

[11] M. Roger, Phys. Rev. Lett. **64**, 297 (1990).

[12] M. Siqueira, J. Nyéki, B. P. Cowan, and J. Saunders, Phys. Rev. Lett. **78**, 2600 (1997).

[13] M. Roger, Phys. Rev. B **56**, R2928 (1997).

[14] K.-D. Morhard *et al.,* Phys. Rev. B **53**, 2658 (1996).

[15] *Phase Transitions and Critical Phenomena,* edited by C. Domb and M. S. Green (Academic, London, 1974), Vol. 3; (1989), Vol. 13.

[16] P. Kopietz *et al.,* Europhys. Lett. **9**, 495 (1989).

[17] M. Roger (to be published).

[18] M. Roger *et al.* (to be published).

[19] S. W. Van Sciver, Phys. Rev. B **18**, 277 (1978).

[20] The analysis of Greywall's specific heat data in the Heisenberg regime ($0.22 < x < 0.32$) with an improved estimate of $\rho_2(x)$, gives a similar value: $\Gamma_{J_c} \approx 25$ [18].